Pex3 confines pexophagy receptor activity of Atg36 to peroxisomes by regulating Hrr25-mediated phosphorylation and proteasomal degradation

Received for publication, March 23, 2020, and in revised form, August 9, 2020 Published, Papers in Press, September 21, 2020, DOI 10.1074/jbc.RA120.013565

Sota Meguro, Xizhen Zhuang, Hiromi Kirisako, and Hitoshi Nakatogawa*

From the School of Life Science and Technology, Tokyo Institute of Technology, Yokohama, Japan

Edited by George N. DeMartino

In macroautophagy (hereafter autophagy), cytoplasmic molecules and organelles are randomly or selectively sequestered within double-membrane vesicles called autophagosomes and delivered to lysosomes or vacuoles for degradation. In selective autophagy, the specificity of degradation targets is determined by autophagy receptors. In the budding yeast *Saccharomyces cerevisiae*, autophagy receptors interact with specific targets and Atg11, resulting in the recruitment of a protein complex that initiates autophagosome formation. Previous studies have revealed that autophagy receptors are regulated by posttranslational modifications. In selective autophagy of peroxisomes (pexophagy), the receptor Atg36 localizes to peroxisomes by binding to the peroxisomal membrane protein Pex3. We previously reported that Atg36 is phosphorylated by Hrr25 (casein kinase 1δ), increasing the Atg36–Atg11 interaction and thereby stimulating pexophagy initiation. However, the regulatory mechanisms underlying Atg36 phosphorylation are unknown. Here, we show that Atg36 phosphorylation is abolished in cells lacking Pex3 or expressing a Pex3 mutant defective in the interaction with Atg36, suggesting that the interaction with Pex3 is essential for the Hrr25-mediated phosphorylation of Atg36. Using recombinant proteins, we further demonstrated that Pex3 directly promotes Atg36 phosphorylation by Hrr25. A co-immunoprecipitation analysis revealed that the interaction of Atg36 with Hrr25 depends on Pex3. These results suggest that Pex3 increases the Atg36–Hrr25 interaction and thereby stimulates Atg36 phosphorylation on the peroxisomal membrane. In addition, we found that Pex3 binding protects Atg36 from proteasomal degradation. Thus, Pex3 confines Atg36 activity to the peroxisome by enhancing its phosphorylation and stability on this organelle.

Macroautophagy (hereafter autophagy) is a highly conserved lysosomal or vacuolar degradation system in eukaryotes (1, 2). In autophagy, cytoplasmic molecules and organelles are sequestered into double-membrane vesicles called autophagosomes, delivered to lysosomes or vacuoles, and degraded by hydrolases within these organelles. Autophagy nonselectively degrades these cellular components to promote their turnover and to supply degradation products as nutrients under starvation conditions (3, 4). In addition, autophagy selectively eliminates proteins or organelles that have become unnecessary or detrimental for cells (5). Recent studies have suggested that degradation of aberrant proteins, mitochondria, and the endoplasmic reticulum by selective autophagy is closely related to neuronal diseases in humans (6).

Previous studies have identified over 40 autophagy-related (Atg) proteins, including core Atg proteins involved in autophagosome biogenesis (7) and autophagy receptors involved in the recognition of degradation targets during selective autophagy (5, 8, 9). Autophagy receptors in yeast bind to degradation targets and interact with Atg11, which recruits core Atg proteins to initiate autophagosome formation in the vicinity of the targets (10). Similarly, some mammalian autophagy receptors, such as p62/SQSTM1 and CCPG1, interact with FIP200, a component of the autophagy-initiation complex (11, 12). In the budding yeast *Saccharomyces cerevisiae*, Atg19, Atg32, Atg34, Atg36, Atg39, Atg40, and Cue5 act as autophagy receptors, which target vacuolar enzymes, mitochondria, α-mannosidase (Ams1), peroxisomes, the nucleus, the endoplasmic reticulum, and polyQ proteins, respectively (13–21).

Selective autophagy should be tightly regulated to avoid undesirable degradation, and most autophagy receptors are regulated by posttranslational modifications (5). In yeast, the mitophagy receptor Atg32 is phosphorylated by casein kinase 2, resulting in increased Atg32–Atg11 interactions and thereby the stimulation of mitophagy initiation (22, 23). Moreover, we and another group have reported that the cytoplasm-to-vacuole targeting pathway (vacuolar enzyme transport via the autophagy machinery), the Ams1 pathway, and pexophagy (selective autophagy of peroxisomes) are regulated in a similar manner (24–26). The receptors Atg19, Atg34, and Atg36 are phosphorylated by the casein kinase 1δ Hrr25, and their increased interactions with Atg11 promote the corresponding pathways.

In *S. cerevisiae*, peroxisomes proliferate during growth in oleate medium, in which peroxisomal functions are important for cells. A previous study has shown that Atg36-dependent pexophagy is induced by long-term culture in oleate media or by exchanging the medium to nitrogen starvation medium containing glucose (19). In addition, Atg36 is expressed during cell culture in oleate medium and localizes to peroxisomes via the interaction with the peroxisomal membrane protein Pex3. Moreover, Atg36 is phosphorylated by Hrr25, and this phosphorylation promotes the Atg36–Atg11 interaction and triggers pexophagy (24). However, the mechanisms underlying pexophagy regulation are still poorly understood.

This article contains supporting information.

* For correspondence: Hitoshi Nakatogawa, hnakatogawa@bio.titech.ac.jp.

In this study, we reveal two distinct mechanisms by which Atg36 activity is confined to peroxisomes: Proteasomal degradation of cytoplasmic Atg36 and Hrr25-mediated activation of peroxisomal Atg36. In both mechanisms, Pex3 acts as a molecular switch.

Results

Pex3 is involved in the phosphorylation of Atg36

A previous study has shown that the peroxisomal membrane protein Pex3 recruits Atg36 to peroxisomes during pexophagy (19). GFP-tagged Atg36 was detected as multiple bands, mostly representing the protein phosphorylated by Hrr25, under pexophagy-inducing conditions (nitrogen starvation following cell growth in oleate medium) (24) (Fig. 1*A*). To analyze the phosphorylation of Atg36-GFP, the *ATG1* gene, which encodes a protein kinase responsible for autophagosome formation, was knocked out to block degradation of Atg36-GFP via pexophagy. We found that Atg36 phosphorylation was almost completely lost when *PEX3* was disrupted (Fig. 1*A*). Pex3 is a peroxin responsible for the biogenesis of peroxisomes (27). To examine whether peroxisome biogenesis is important for Atg36 phosphorylation, we knocked out other peroxin genes, *PEX1*, *PEX5*, *PEX11*, *PEX14*, and *PEX19*. Unlike the results for the knockout of *PEX3*, the phosphorylation of Atg36-GFP was not substantially impaired by the knockout of these *PEX* genes (Fig. 1*B*). These results suggest that Atg36 phosphorylation by Hrr25 requires Pex3, independent of its function in peroxisome biogenesis.

Atg36 phosphorylation requires the interaction with Pex3

Next, we investigated whether the interaction of Atg36 with Pex3 is required for Atg36 phosphorylation by Hrr25. WT Pex3 and the Pex3-177 mutant, which is functional for peroxisome biogenesis but is defective in Atg36 binding (19), were fused with mCherry and expressed from single-copy plasmids in *PEX3* knockout cells. The phosphorylation of Atg36-GFP was observed in cells expressing WT Pex3-mCherry but was decreased in cells expressing Pex3-177–mCherry (Fig. 1*C*), suggesting that the binding of Atg36 to Pex3 is important for Atg36 phosphorylation by Hrr25.

We investigated whether the Atg36–Pex3 interaction on the peroxisome is required for Atg36 phosphorylation. Pex3, which consists of 441 amino acid residues, is anchored to the peroxisomal membrane by its N-terminal transmembrane domain (28). Chromosomal *PEX3* was engineered to express Pex3-mCherry lacking the transmembrane domain ($Pex3^{40–441}$-mCherry). In addition, because the protein level of $Pex3^{40–441}$-mCherry was lower than that of WT Pex3-mCherry, the promoter was replaced with the *ADH1* promoter to increase the protein level to that of WT Pex3-mCherry expressed under the original promoter (Fig. 1*D*). We also confirmed that whereas WT Pex3-mCherry and Atg36-GFP colocalized at peroxisomes (cells expressing Atg36-GFP contain a few clusters of peroxisomes) (19), $Pex3^{40–441}$-mCherry and Atg36-GFP were both dispersed throughout the cytoplasm (Fig. 1*E*). $Pex3^{40–441}$-mCherry and WT Pex3-mCherry resulted in similar levels of Atg36-GFP phosphorylation (Fig. 1*D*). These results suggest that the Atg36–Pex3 interaction *per se* is important for Atg36 phosphorylation by Hrr25 and does not need to occur on the peroxisome.

Pex3 directly promotes Atg36 phosphorylation by Hrr25

Our previous *in vitro* kinase assay using recombinant Hrr25 and GST-tagged Atg36 demonstrated that Hrr25 directly phosphorylates Atg36 (24). The cytoplasmic region of Pex3 ($Pex3^{40–441}$) was purified and added to this *in vitro* reaction. When GST-Atg36 was incubated with Hrr25 and ATP in the absence of $Pex3^{40–441}$, the band of GST-Atg36 was slightly upshifted (Fig. 2*A*). The addition of $Pex3^{40–441}$ to the reaction caused upshifted bands of most GST-Atg36. The upshifted band of GST-Atg36 disappeared by treatment with λ protein phosphatase, and the disappearance was impeded by phosphatase inhibitors (Fig. 2*B*). Moreover, Pex3-$177^{40–441}$, which is defective in the interaction with Atg36, had no effect on the band shift of GST-Atg36 by Hrr25 (Fig. 2*A*). These results demonstrated that Pex3 interacts with Atg36 and directly promotes its phosphorylation by Hrr25.

Pex3 enhances the interaction of Atg36 with Hrr25

Previous studies have shown that Atg36 interacts with Pex3 (19) and that Hrr25 is dispensable for the interaction (24). Consistent with the fact that Atg36 is a substrate of Hrr25, immunoprecipitation of Hrr25-GFP coprecipitated Atg36-myc (Fig. 3*A*). This coprecipitation depended on Pex3, suggesting that Pex3 increases the interaction of Atg36 with Hrr25. Furthermore, Pex3-myc was co-immunoprecipitated with Hrr25-GFP, and *ATG36* knockout abolished this coprecipitation (Fig. 3*B*). These results suggest that Pex3 directly interacts with Hrr25 in association with Atg36 or indirectly interacts with Hrr25 via Atg36.

Pex3 protects Atg36 from proteasomal degradation

We noticed that, in addition to the decrease in phosphorylation, the protein levels of Atg36 were substantially lower in cells lacking Pex3 (Fig. 1, *A* and *B*) or expressing the Pex3-177 mutant deficient for the interaction with Atg36 than in cells with WT Pex3 (Fig. 1*C*). In addition, Atg36 levels were almost normal in the presence of cytoplasmically expressed Pex3 ($Pex3^{41–441}$) (Fig. 1*D*). These results suggested that Pex3 binding is important for not only the Hrr25-mediated phosphorylation of Atg36 but also the protein stability of Atg36. We found that the treatment of *PEX3* knockout cells with the proteasome inhibitor MG132 substantially increased Atg36-GFP in both oleate and nitrogen starvation media, suggesting that Atg36 is susceptible to degradation by the proteasome in the absence of Pex3 (Fig. 4*A*). MG132 also increased Atg36-GFP in *pex3-177* cells (Fig. 4*B*), and it had a weaker effect on Atg36-GFP levels in cells expressing WT Pex3 (Fig. 4, *A* and *B*). These results suggest that Pex3 binding to Atg36 blocks proteasomal degradation of Atg36.

Discussion

In this study, we investigated the mechanisms underlying pexophagy regulation, with a focus on the pexophagy receptor

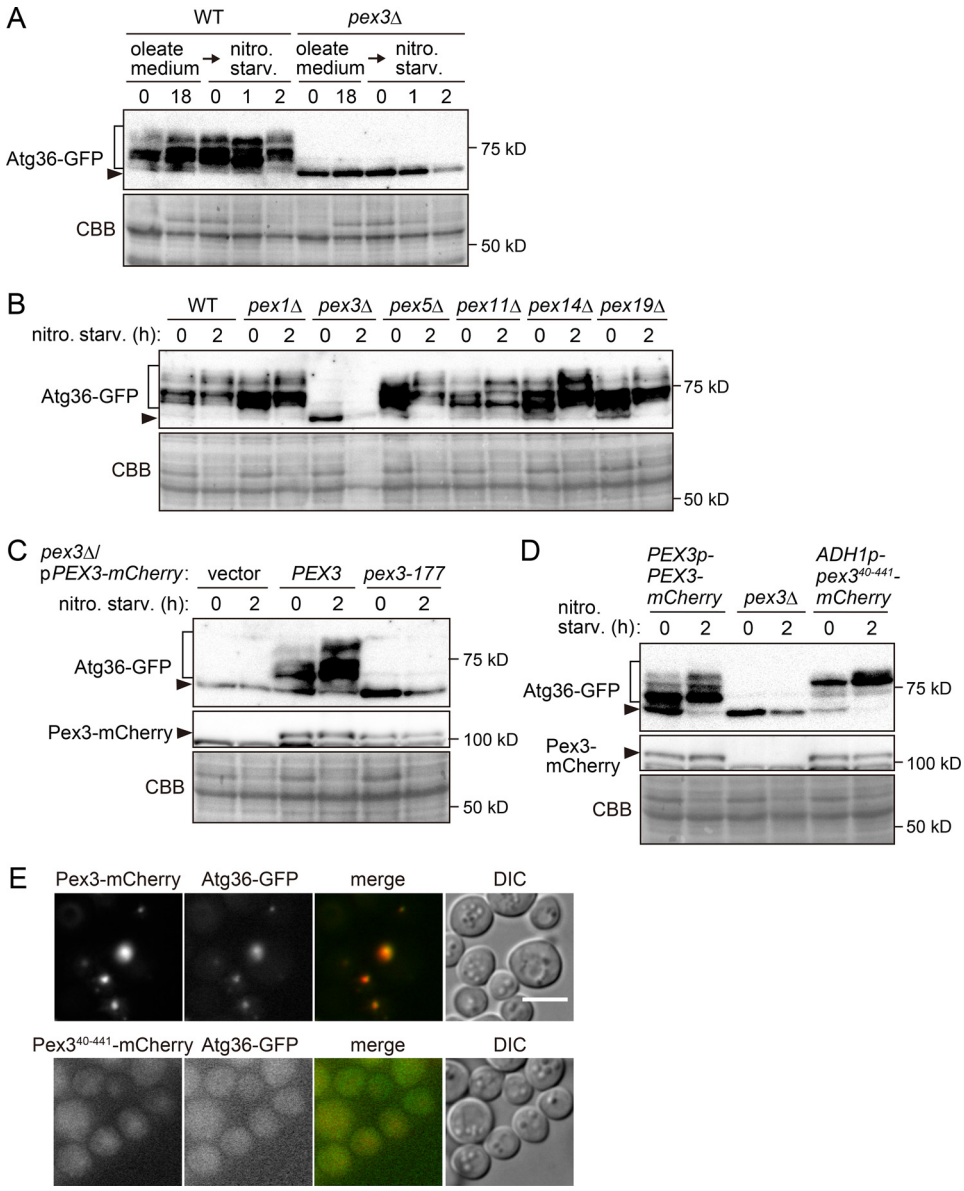

Figure 1. Pex3 is indispensable for the phosphorylation of Atg36. *A* and *B*, *ATG36-GFP atg1*Δ cells grown in glucose media were shifted to oleate medium for 18 h and then incubated in nitrogen starvation medium. The phosphorylation of Atg36-GFP was examined by immunoblotting using an anti-GFP antibody. The *square bracket and arrow head* indicate phosphorylated and unphosphorylated Atg36-GFP, respectively. *C*, phosphorylation of Atg36-GFP in *atg1*Δ *pex3*Δ cells carrying single-copy plasmids expressing Pex3-mCherry or Pex3-177-mCherry was examined as described in *A*. Levels of Pex3-mCherry were checked by immunoblotting using anti-RFP antibodies. *D*, phosphorylation of Atg36-GFP and Pex3-mCherry levels in *atg1*Δ cells expressing Pex3-mCherry with the original promoter or Pex3$^{40–441}$-mCherry with the *ADH1* promoter were examined as described in *A* and *C*. *E*, the same strains described in *D* were grown in oleate medium for 18 h, subjected to nitrogen starvation for 2 h, and the subcellular localization of Atg36-GFP and Pex3-mCherry was observed under a fluorescence microscope. DIC, differential interference contrast microscopy. *Scale bar*, 5 μM.

Atg36. We first showed that Pex3 is involved in the Hrr25-mediated phosphorylation of Atg36, independent of peroxisome biogenesis and the localization of these proteins to peroxisomes (Fig. 1). *In vitro* analysis using recombinant proteins revealed that Pex3 directly promotes Atg36 phosphorylation by Hrr25 (Fig. 2). Moreover, co-immunoprecipitation analysis suggested that the interaction of Atg36 with Hrr25 is enhanced by Pex3 and that Hrr25 directly or indirectly interacts with Pex3 depending on Atg36 (Fig. 3). These results allow us to propose a model for the spatial regulation of Atg36 phosphorylation by Hrr25 (Fig. 5). Although cytoplasmic Atg36 is not a good substrate for Hrr25, it becomes efficiently phosphorylated by Hrr25 when bound to Pex3 in the peroxisomal membrane. Pex3 and Atg36 may both interact with Hrr25 to retain the kinase at the complex, facilitating Atg36 phosphorylation by Hrr25 (Fig. 5*i*). Alternatively, Pex3 binding may induce a conformational change in Atg36, increasing Atg36 affinity to Hrr25 (Fig. 5*ii*). The conformational change may also increase the accessibility of Hrr25 to phosphorylation sites in Atg36. Pex3-dependent phosphorylation clearly enables the specific activation of Atg36 that has been correctly localized to the peroxisome as a degradation target.

In the methylotrophic yeast *Komagataella phaffii* (formerly *Pichia pastoris*), Atg30 functions as a pexophagy receptor

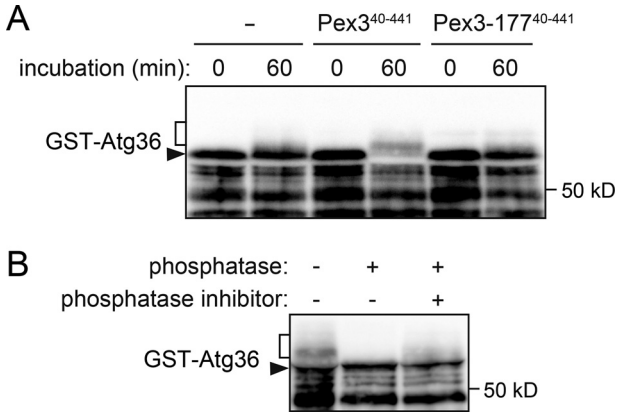

Figure 2. Pex3 directly promotes Atg36 phosphorylation by Hrr25. *A*, recombinant GST-Atg36 was incubated with Hrr25 and ATP in the presence or absence of Pex3$^{40–441}$ or Pex3-177$^{40–441}$ at 30°C, and the phosphorylation of GST-Atg36 was examined by immunoblotting using an anti-GST antibody. *B*, recombinant GST-Atg36 incubated with Hrr25, Pex3$^{40–441}$, and ATP for 60 min was treated with λ protein phosphatase in the presence or absence of phosphatase inhibitors and analyzed by immunoblotting using an anti-GST antibody.

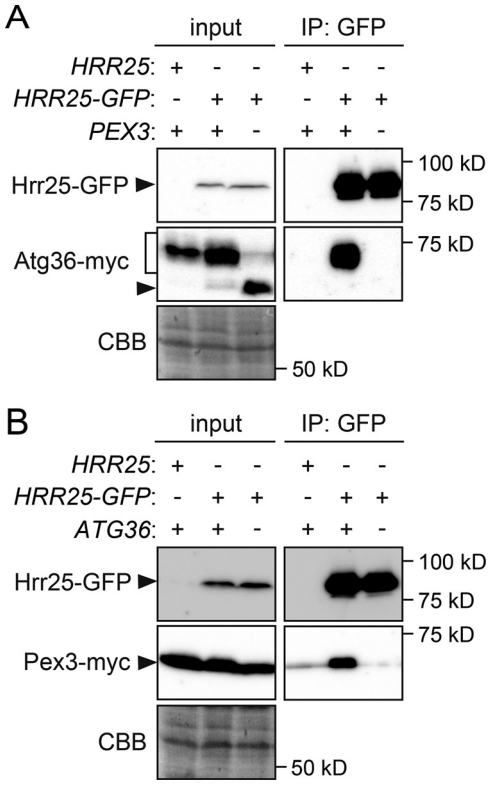

Figure 3. Pex3 increases the interaction of Atg36 with Hrr25. Cells expressing Hrr25-GFP and Atg36-myc (*A*) or Pex3-myc (*B*) grown in oleate medium were starved of nitrogen for 2 h, and the cell lysates (*input*) were subjected to immunoprecipitation using an anti-GFP antibody. The immunoprecipitates (*IP*) were analyzed by immunoblotting using antibodies against GFP and the myc sequence.

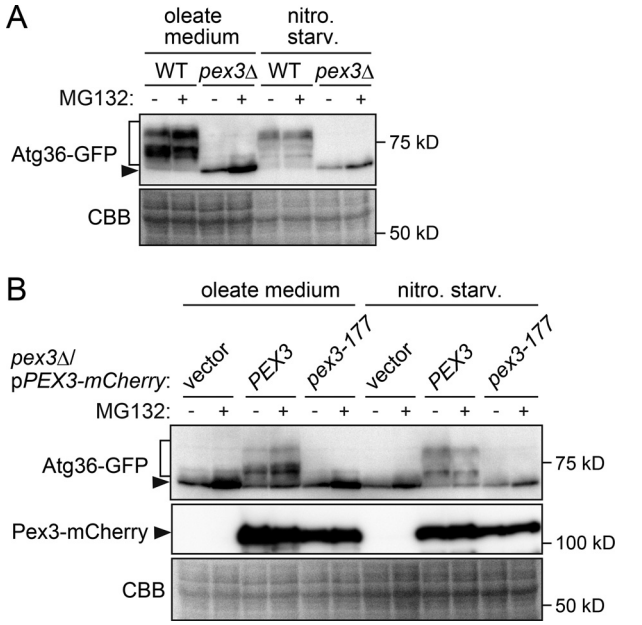

Figure 4. Atg36 not associated with Pex3 is susceptible to proteasomal degradation. *A*, *ATG36-GFP atg1Δ erg6Δ* cells (in which *ERG6* was knocked out for efficient proteasome inhibition by MG132) were grown in oleate medium for 18 h. These cells were treated with or without MG132 in oleate medium or nitrogen starvation medium for 4 h and examined by immunoblotting using an anti-GFP antibody. *B*, proteasomal degradation of Atg36-GFP in *atg1Δ erg6Δ pex3Δ* cells carrying Pex3-mCherry or Pex3-177-mCherry plasmids was examined as described in *A*. Pex3-mCherry levels were also checked by immunoblotting using anti-RFP antibodies.

(29). Despite no sequence similarity between Atg30 and Atg36, these proteins share a number of functional characteristics. Similar to Atg36, Atg30 is recruited to peroxisomes by interacting with Pex3 (30). In addition, Atg30 is also phosphorylated by Hrr25, and this phosphorylation is likely to increase the Atg30 interaction with Atg11 (29–31). However, unlike in *S. cerevisiae*, Pex3 and Hrr25 competitively bind to Atg30 and therefore Pex3 inhibits the Hrr25-mediated phosphorylation of Atg30 (31). Instead, in *K. phaffii*, the peroxisomal acyl-CoA–binding protein Atg37 has been proposed to promote the phosphorylation of Atg30 by Hrr25 (31, 32). Thus, although details are different, these two yeast species both evolved mechanisms to specifically activate pexophagy receptors localized to peroxisomes. Of note, recent studies have shown that mammalian cells regulate pexophagy in a different manner; ubiquitination of peroxisomal proteins, including peroxins, recruits ubiquitin-binding autophagy adaptors, such as p62/SQSTM1 and NBR1, to peroxisomes, leading to their sequestration into autophagosomes (33, 34).

In this study, we also found that cytoplasmic Atg36 (Atg36 not associated with Pex3) is susceptible to degradation by the proteasome (Fig. 4). Pex3 may mask a degron sequence in Atg36. Alternatively, phosphorylation by Hrr25 following Pex3 binding may affect Atg36 recognition by an unknown factor that directs Atg36 to proteasomal degradation. Degradation of cytoplasmic Atg36 can also contribute to the confinement of Atg36 activity to peroxisomes (Fig. 5). In addition, it may prevent excess pexophagy. A previous study has reported that the absence of the exportomer subunit Pex1 increases the protein level and phosphorylation of Atg36 and stimulates pexophagy (35). These results suggest that specific changes in peroxisomes affect the phosphorylation and stability of Atg36 on the peroxisome and are linked to pexophagy regulation. Future studies will elucidate the mechanism underlying Atg36 degradation, including the identification of a degron sequence in Atg36 and an E3 ligase responsible for the ubiquitination of Atg36.

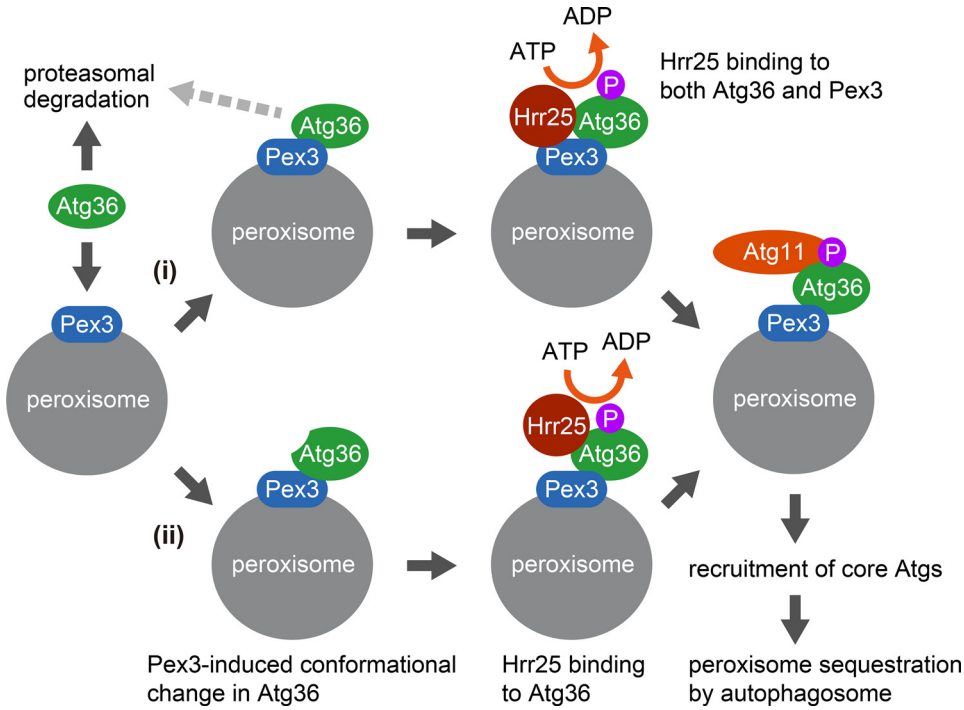

Figure 5. Two mechanisms by which Pex3 confines Atg36 activity to peroxisomes. Cytoplasmic (nonperoxisomal) Atg36 is not efficiently phosphorylated by Hrr25. Pex3 not only plays a role in the peroxisomal localization of Atg36, but also increases the interaction of Atg36 with Hrr25 and thereby stimulates the phosphorylation of Atg36 on peroxisomes. We propose two mechanisms to explain this pattern: (*i*) Pex3 and Atg36 cooperatively bind to Hrr25 or (*ii*) Pex3 induces a conformational change in Atg36, increasing its affinity to Hrr25. In addition, cytoplasmic Atg36, but not Pex3-bound Atg36, is subject to degradation by the proteasome. Thus, both the phosphorylation and stability of Atg36 are enhanced by Pex3, and thereby Atg36 activity is confined to peroxisomes.

Experimental Procedures

Yeast strains and media

The yeast strains used in this study are listed in Table S1. Gene disruption and tagging were performed by a PCR-based method (36). Yeast cells were grown in SD+CA+ATU medium (0.17% yeast nitrogen base without amino acids and ammonium sulfate (YNB w/o aa and as), 0.5% ammonium sulfate, 2% glucose, 0.5% casamino acids, 0.002% adenyl sulfate, 0.002% tryptophan, and 0.002% uracil) at 30°C. Cells carrying pRS316-derived plasmids were cultured in SD+CA+ATU medium without uracil. To induce pexophagy, cells were grown in these media for 24 h (A_{600} reached ~6), diluted 10-fold with SO+CA+ATU medium (0.17% YNB w/o aa and as, 0.5% ammonium sulfate, 0.1% glucose, 0.12% oleate, 0.2% Tween 40, 1% casamino acids, 0.1% yeast extract, 0.002% adenine sulfate, 0.002% tryptophan, and 0.002% uracil), and grown for 18 h (A_{600} reached ~4; cells lacking *PEX* genes grew normally during this time period probably because SO+CA+ATU medium contained 0.1% glucose), and the medium was replaced with SD-N (0.17% YNB w/o aa and as and 2% glucose). 20 mM MG132 dissolved in DMSO was added to the media to a final concentration of 100 μM for proteasome inhibition.

Plasmids

Oligonucleotides used for plasmid construction are listed in Table S2. The pGEX-6P-Pex3$^{40–441}$ plasmid for GST-Pex3$^{40–441}$ expression in *Escherichia coli* was constructed as follows. The DNA sequence encoding Pex3$^{40–441}$ was amplified by PCR using genomic DNA from BY4741 (37) and the oligonucleotides Pex3$^{40–441}$ forward and reverse. Products were cloned into the pGEX-6P-1 vector (GE Healthcare) using BamHI and EcoRI. The *pex3-177* mutation (F64S,T74A,H354L) (19) was introduced into this plasmid using the QuikChange Site-Directed Mutagenesis Kit (Agilent) in two steps with the pairs of oligonucleotides Pex3 F64ST74A forward and reverse and Pex3 H354L forward and reverse, resulting in pGEX-6P-Pex3-177$^{40–441}$. pGEX-6P-Atg36 and pGEX-6P-Hrr25 have been described previously (24). To construct the plasmid expressing Pex3-2×mCherry (pRS316-*PEX3-2×mCherry*), the *PEX3-2×mCherry* sequence with the *PEX3* promoter and the *PGK1* terminator was amplified by PCR using genomic DNA from YMS28 and the oligonucleotides Pex3-2mCherry 500 bp up and Pex3-2mCherry-PGKter down, and cloned into the single-copy vector pRS316 using BamHI and EcoRI. The *pex3-177* mutation was introduced into this plasmid as described above to construct pRS316-*pex3-177*$^{40–441}$*-2×mCherry*.

Immunoblotting

Yeast cell pellets (~3–6 A_{600} units) were suspended in 200 μl of water, mixed with 200 μl of 0.2 M NaOH, stayed at room temperature for 5 min, and centrifuged at 5000 × *g* for 5 min at 4°C. The pellets were suspended in (5 × A_{600} units) μl of 2× urea sample buffer (75 mM MOPS-NaOH, pH 6.8, 4% SDS, 8 M urea, and 200 mM DTT) by vortexing at 65°C for 5 min and centrifuged at 15,000 × *g* for 1 min, and the supernatants were used for immunoblotting. Monoclonal antibodies against GFP (JL-8; Clontech), mCherry (a gift from Dr. Toshiya Endo), GST (B-14; Santa Cruz Biotechnology), and myc (9E10; Santa Cruz Biotechnology) were used for the detection of tagged proteins.

Fluorescence microscopy

Fluorescence microscopy was performed as described previously (38) using an inverted fluorescence microscope (IX83; Olympus) equipped with an electron-multiplying charged coupled device camera (ImagEM C9100-13; Hamamatsu Photonics), a 150 objective lens (UAPON 150XOTIRF, NA/1.45; Olympus), a 488 nm blue laser (50 milliwatt; Coherent) for GFP excitation, and a 588 nm yellow laser (50 milliwatt; Coherent) for mCherry excitation. MetaMorph (Molecular Devices) and Fiji (ImageJ) (39, 40) were used for image acquisition and processing, respectively.

Protein purification

GST-Atg36, Hrr25, Pex3$^{40–441}$, Pex3-177$^{40–441}$ were purified as described previously (41). Briefly, *E. coli* BL21 cells carrying pGEX-6P–based plasmids expressing GST-fused Atg36, Hrr25, Pex3$^{40–441}$, or Pex3-177$^{40–441}$ were grown in LB medium (10 mg/ml tryptone, 5 mg/ml yeast extract, 10 mg/ml NaCl, and 1 mM NaOH) containing 50 μg/ml ampicillin, and treated with 0.1 mM isopropyl-β-D-thiogalactopyranoside at 16°C for 18 h. Cell pellets were suspended in buffer B (20 mM HEPES-KOH, pH 7.2, and 150 mM NaCl) containing 5 mM DTT, 0.5 mM ethylenediaminetetraacetic acid, and 0.1 mM phenylmethylsulfonyl fluoride. The lysates were prepared as described previously (41) and rotated with GSH-Sepharose 4B resin (GE Healthcare) at 4°C for 45 min. The resins were washed with buffer B, and GST-Atg36 was eluted with 50 mM Tris-HCl, pH 8.0, containing 150 mM NaCl and 10 mM reduced GSH. To elute GST-free Hrr25, Pex3$^{40–441}$, and Pex3-177$^{40–441}$, the resins were treated with the PreScission Protease (GE Healthcare), which cleaves the linker between GST and the fused proteins. The purified proteins were concentrated using Vivaspin 6000–10,000 columns (Sartorius), supplemented with glycerol at a final concentration of 25%, and stored at −80°C.

In vitro kinase assay

0.3 μM GST-Atg36 was incubated with 0.05 μM Hrr25 at 30°C in the presence or absence of 3 μM Pex3$^{40–441}$ or Pex3-177$^{40–441}$ in 20 mM HEPES-KOH, pH 7.2, containing 150 mM NaCl, 1 mM $MgCl_2$, 0.2 mM DTT, and 1 mM ATP.

Phosphatase treatment

After *in vitro* phosphorylation reactions, samples were incubated with λ protein phosphatase (New England Biolabs) in NEBuffer Pack for Protein MetalloPhosphatases containing 1 mM $MgCl_2$ at 30°C for 1 h in the presence or absence of PhosSTOP phosphatase inhibitor mixture (Roche).

Immunoprecipitation

Yeast cells were disrupted in buffer A (50 mM Tris-HCl, pH 8.0, 150 mM NaCl, and 10% sorbitol) containing 2 mM phenylmethylsulfonyl fluoride and 2× protease inhibitor mixture (cOmplete, EDTA-free; Roche) using a Multi-beads Shocker (Yasui Kikai) and 0.5-mm YZB zirconia beads. The lysates were treated with 0.5% Triton X-100 at 4°C for 30 min on a rotator, and centrifuged at 15,000 × *g* for 15 min. The supernatants were mixed with GFP-nanobody (GFP-binding protein)–conjugated magnetic beads (42) and rotated at 4°C for 2 h. The beads were washed with buffer A, and the bound proteins were eluted by mixing the beads in SDS sample buffer (50 mM Tris-HCl, pH 7.5, 2% SDS, 8% glycerol, 20 mM DTT) at 65°C for 5 min.

Data availability

All of the data are contained within the manuscript.

Acknowledgments—We thank our laboratory members for materials, discussions, and technical and secretarial support; Dr. Toshiya Endo for antibodies against mCherry (RFP); and Biomaterials Analysis Division, Open Facility Center at Tokyo Institute of Technology for DNA sequencing service. This work was supported in part by Ministry of Education, Culture, Sports, Science and Technology of Japan KAKENHI Grants-in-Aid for Scientific Research 25111003, 17H01430, and 19H05708 (to H. N.) and by STAR Grant funded by the Tokyo Tech Fund (to H. N.).

Author contributions—S. M. and H. N. conceptualization; S. M., X. Z., and H. K. data curation; S. M. formal analysis; S. M. and H. N. validation; S. M. investigation; S. M. and H. N. writing-original draft; X. Z. and H. K. resources; X. Z., H. K., and H. N. writing-review and editing; H. N. supervision; H. N. funding acquisition; H. N. project administration.

Funding and additional information—This work was supported by the Ministry of Education, Culture, Sports, Science and Technology (MEXT) of Japan, Grants 25111003, 17H01430, and 19H05708 (to H. N.). Support was also provided by Tokyo Tech Fund with a STAR Grant (to H.N).

Conflict of interest—The authors declare that they have no conflicts of interest with the contents of this article.

Abbreviation—The abbreviations used is: YNB w/o aa and as, yeast nitrogen base without amino acids and ammonium sulfate.

References

1. Yang, Z., and Klionsky, D. J. (2010) Eaten alive: A history of macroautophagy. *Nat. Cell Biol.* **12,** 814–822 CrossRef Medline
2. Ohsumi, Y. (2014) Historical landmarks of autophagy research. *Cell Res.* **24,** 9–23 CrossRef Medline
3. Mizushima, N., and Komatsu, M. (2011) Autophagy: Renovation of cells and tissues. *Cell* **147,** 728–741 CrossRef Medline
4. Levine, B., and Klionsky, D. J. (2004) Development by self-digestion: Molecular mechanisms and biological functions of autophagy. *Dev. Cell.* **6,** 463–477 CrossRef Medline
5. Gatica, D., Lahiri, V., and Klionsky, D. J. (2018) Cargo recognition and degradation by selective autophagy. *Nat. Cell Biol.* **20,** 233–242 CrossRef Medline
6. Conway, O., Akpinar, H. A., Rogov, V. V., and Kirkin, V. (2020) Selective autophagy receptors in neuronal health and disease. *J. Mol. Biol.* **432,** 2483–2509 CrossRef Medline
7. Nakatogawa, H. (2020) Mechanisms governing autophagosome biogenesis. *Nat. Rev. Mol. Cell Biol.* **21,** 439–458 CrossRef Medline
8. Stolz, A., Ernst, A., and Dikic, I. (2014) Cargo recognition and trafficking in selective autophagy. *Nat. Cell Biol.* **16,** 495–501 CrossRef Medline

9. Farré, J. C., and Subramani, S. (2016) Mechanistic insights into selective autophagy pathways: Lessons from yeast. *Nat. Rev. Mol. Cell Biol.* **17,** 537–552 CrossRef Medline
10. Zientara-Rytter, K., and Subramani, S. (2020) Mechanistic insights into the role of Atg11 in selective autophagy. *J. Mol. Biol.* **432,** 104–122 CrossRef Medline
11. Smith, M. D., Harley, M. E., Kemp, A. J., Wills, J., Lee, M., Arends, M., von Kriegsheim, A., Behrends, C., and Wilkinson, S. (2018) CCPG1 is a non-canonical autophagy cargo receptor essential for ER-phagy and pancreatic ER proteostasis. *Dev. Cell.* **44,** 217–232.e11 CrossRef Medline
12. Turco, E., Witt, M., Abert, C., Bock-Bierbaum, T., Su, M.-Y., Trapannone, R., Sztacho, M., Danieli, A., Shi, X., Zaffagnini, G., Gamper, A., Schuschnig, M., Fracchiolla, D., Bernklau, D., Romanov, J., *et al.* (2019) FIP200 claw domain binding to p62 promotes autophagosome formation at ubiquitin condensates. *Mol. Cell.* **74,** 330–346.e11 CrossRef Medline
13. Scott, S. V., Guan, J., Hutchins, M. U., Kim, J., and Klionsky, D. J. (2001) Cvt19 is a receptor for the cytoplasm-to-vacuole targeting pathway. *Mol. Cell.* **7,** 1131–1141 CrossRef Medline
14. Yuga, M., Gomi, K., Klionsky, D. J., and Shintani, T. (2011) Aspartyl aminopeptidase is imported from the cytoplasm to the vacuole by selective autophagy in *Saccharomyces cerevisiae*. *J. Biol. Chem.* **286,** 13704–13713 CrossRef Medline
15. Kageyama, T., Suzuki, K., and Ohsumi, Y. (2009) Lap3 is a selective target of autophagy in yeast, *Saccharomyces cerevisiae*. *Biochem. Biophys. Res. Commun.* **378,** 551–557 CrossRef Medline
16. Kanki, T., Wang, K., Cao, Y., Baba, M., and Klionsky, D. J. (2009) Atg32 is a mitochondrial protein that confers selectivity during mitophagy. *Dev. Cell.* **17,** 98–109 CrossRef Medline
17. Okamoto, K., Kondo-Okamoto, N., and Ohsumi, Y. (2009) Mitochondria-anchored receptor Atg32 mediates degradation of mitochondria via selective autophagy. *Dev. Cell.* **17,** 87–97 CrossRef Medline
18. Suzuki, K., Kondo, C., Morimoto, M., and Ohsumi, Y. (2010) Selective transport of α-mannosidase by autophagic pathways: Identification of a novel receptor, Atg34p. *J. Biol. Chem.* **285,** 30019–30025 CrossRef Medline
19. Motley, A. M., Nuttall, J. M., and Hettema, E. H. (2012) Pex3-anchored Atg36 tags peroxisomes for degradation in *Saccharomyces cerevisiae*. *EMBO J.* **31,** 2852–2868 CrossRef Medline
20. Mochida, K., Oikawa, Y., Kimura, Y., Kirisako, H., Hirano, H., Ohsumi, Y., and Nakatogawa, H. (2015) Receptor-mediated selective autophagy degrades the endoplasmic reticulum and the nucleus. *Nature* **522,** 359–362 CrossRef Medline
21. Lu, K., Psakhye, I., and Jentsch, S. (2014) Autophagic clearance of PolyQ proteins mediated by ubiquitin-Atg8 adaptors of the conserved CUET protein family. *Cell* **158,** 549–563 CrossRef Medline
22. Kanki, T., Kurihara, Y., Jin, X., Goda, T., Ono, Y., Aihara, M., Hirota, Y., Saigusa, T., Aoki, Y., Uchiumi, T., and Kang, D. (2013) Casein kinase 2 is essential for mitophagy. *EMBO Rep.* **14,** 788–794 CrossRef Medline
23. Aoki, Y., Kanki, T., Hirota, Y., Kurihara, Y., Saigusa, T., Uchiumi, T., and Kang, D. (2011) Phosphorylation of serine 114 on Atg32 mediates mitophagy. *Mol. Biol. Cell* **22,** 3206–3217 CrossRef Medline
24. Tanaka, C., Tan, L. J., Mochida, K., Kirisako, H., Koizumi, M., Asai, E., Sakoh-Nakatogawa, M., Ohsumi, Y., and Nakatogawa, H. (2014) Hrr25 triggers selective autophagy-related pathways by phosphorylating receptor proteins. *J. Cell Biol.* **207,** 91–105 CrossRef Medline
25. Mochida, K., Ohsumi, Y., and Nakatogawa, H. (2014) Hrr25 phosphorylates the autophagic receptor Atg34 to promote vacuolar transport of α-mannosidase under nitrogen starvation conditions. *FEBS Lett.* **588,** 3862–3869 CrossRef Medline
26. Pfaffenwimmer, T., Reiter, W., Brach, T., Nogellova, V., Papinski, D., Schuschnig, M., Abert, C., Ammerer, G., Martens, S., and Kraft, C. (2014) Hrr25 kinase promotes selective autophagy by phosphorylating the cargo receptor Atg19. *EMBO Rep.* **15,** 862–870 CrossRef Medline
27. Farré, J. C., Mahalingam, S. S., Proietto, M., and Subramani, S. (2019) Peroxisome biogenesis, membrane contact sites, and quality control. *EMBO Rep.* **20,** e46864 CrossRef Medline
28. Höhfeld, J., Veenhuis, M., and Kunau, W. H. (1991) PAS3, a *Saccharomyces cerevisiae* gene encoding a peroxisomal integral membrane protein essential for peroxisome biogenesis. *J. Cell Biol.* **114,** 1167–1178 CrossRef Medline
29. Farré, J. C., Manjithaya, R., Mathewson, R. D., and Subramani, S. (2008) PpAtg30 tags peroxisomes for turnover by selective autophagy. *Dev. Cell.* **14,** 365–376 CrossRef Medline
30. Burnett, S. F., Farré, J. C., Nazarko, T. Y., and Subramani, S. (2015) Peroxisomal Pex3 activates selective autophagy of peroxisomes via interaction with the pexophagy receptor Atg30. *J. Biol. Chem.* **290,** 8623–8631 CrossRef Medline
31. Zientara-Rytter, K., Ozeki, K., Nazarko, T. Y., and Subramani, S. (2018) Pex3 and Atg37 compete to regulate the interaction between the pexophagy receptor, Atg30, and the Hrr25 kinase. *Autophagy* **14,** 368–384 CrossRef Medline
32. Nazarko, T. Y., Ozeki, K., Till, A., Ramakrishnan, G., Lotfi, P., Yan, M., and Subramani, S. (2014) Peroxisomal Atg37 binds Atg30 or palmitoyl-CoA to regulate phagophore formation during pexophagy. *J. Cell Biol.* **204,** 541–557 CrossRef Medline
33. Cho, D. H., Kim, Y. S., Jo, D. S., Choe, S. K., and Jo, E. K. (2018) Pexophagy: Molecular mechanisms and implications for health and diseases. *Mol. Cells* **41,** 55–64 CrossRef Medline
34. Honsho, M., Yamashita, S. I., and Fujiki, Y. (2016) Peroxisome homeostasis: Mechanisms of division and selective degradation of peroxisomes in mammals. *Biochim. Biophys. Acta* **1863,** 984–991 CrossRef Medline
35. Nuttall, J. M., Motley, A. M., and Hettema, E. H. (2014) Deficiency of the exportomer components Pex1, Pex6, and Pex15 causes enhanced pexophagy in *Saccharomyces cerevisiae*. *Autophagy* **10,** 835–845 CrossRef Medline
36. Janke, C., Magiera, M. M., Rathfelder, N., Taxis, C., Reber, S., Maekawa, H., Moreno-Borchart, A., Doenges, G., Schwob, E., Schiebel, E., and Knop, M. (2004) A versatile toolbox for PCR-based tagging of yeast genes: New fluorescent proteins, more. *Yeast* **21,** 947–962 CrossRef Medline
37. Brachmann, C. B., Davies, A., Cost, G. J., Caputo, E., Li, J., Hieter, P., and Boeke, J. D. (1998) Designer deletion strains derived from *Saccharomyces cerevisiae* S288C: A useful set of strains and plasmids for PCR-mediated gene disruption and other applications. *Yeast* **14,** 115–132 CrossRef Medline
38. Harada, K., Kotani, T., Kirisako, H., Sakoh-Nakatogawa, M., Oikawa, Y., Kimura, Y., Hirano, H., Yamamoto, H., Ohsumi, Y., and Nakatogawa, H. (2019) Two distinct mechanisms target the autophagy-related e3 complex to the pre-autophagosomal structure. *Elife* **8,** e43088 CrossRef Medline
39. Schindelin, J., Arganda-Carreras, I., Frise, E., Kaynig, V., Longair, M., Pietzsch, T., Preibisch, S., Rueden, C., Saalfeld, S., Schmid, B., Tinevez, J. Y., White, D. J., Hartenstein, V., Eliceiri, K., Tomancak, P., *et al.* (2012) Fiji: An open-source platform for biological-image analysis. *Nat. Methods* **9,** 676–682 CrossRef Medline
40. Schneider, C. A., Rasband, W. S., and Eliceiri, K. W. (2012) NIH Image to ImageJ: 25 years of image analysis. *Nat. Methods* **9,** 671–675 CrossRef Medline
41. Nakatogawa, H., Ichimura, Y., and Ohsumi, Y. (2007) Atg8, a ubiquitin-like protein required for autophagosome formation, mediates membrane tethering and hemifusion. *Cell* **130,** 165–178 CrossRef Medline
42. Kotani, T., Kirisako, H., Koizumi, M., Ohsumi, Y., and Nakatogawa, H. (2018) The Atg2-Atg18 complex tethers pre-autophagosomal membranes to the endoplasmic reticulum for autophagosome formation. *Proc. Natl. Acad. Sci. U. S. A.* **115,** 10363–10368 CrossRef Medline